

Spring-summer temperatures since AD 1780 reconstructed from stable oxygen isotope ratios in white spruce tree-rings from the Mackenzie Delta, northwestern Canada

Trevor J. Porter · Michael F. J. Pisaric · Robert D. Field · Steven V. Kokelj · Thomas W. D. Edwards · Peter deMontigny · Richard Healy · Allegra N. LeGrande

Received: 14 September 2012 / Accepted: 16 January 2013 / Published online: 30 January 2013
© Springer-Verlag Berlin Heidelberg 2013

Abstract High-latitude $\delta^{18}\text{O}$ archives deriving from meteoric water (e.g., tree-rings and ice-cores) can provide valuable information on past temperature variability, but stationarity of temperature signals in these archives depends on the stability of moisture source/trajectory and precipitation seasonality, both of which can be affected by atmospheric circulation changes. A tree-ring $\delta^{18}\text{O}$ record (AD 1780–2003) from the Mackenzie Delta is evaluated as a temperature proxy based on linear regression diagnostics. The primary source of moisture for this region is the North Pacific and, thus, North Pacific atmospheric circulation variability could potentially affect the tree-ring $\delta^{18}\text{O}$ -temperature signal. Over the instrumental period (AD 1892–2003), tree-ring $\delta^{18}\text{O}$ explained 29 % of interannual variability in April–July minimum temperatures, and the explained variability increases substantially at lower-frequencies. A split-period calibration/verification analysis

found the $\delta^{18}\text{O}$ -temperature relation was time-stable, which supported a temperature reconstruction back to AD 1780. The stability of the $\delta^{18}\text{O}$ -temperature signal indirectly implies the study region is insensitive to North Pacific circulation effects, since North Pacific circulation was not constant over the calibration period. Simulations from the NASA-GISS ModelE isotope-enabled general circulation model confirm that meteoric $\delta^{18}\text{O}$ and precipitation seasonality in the study region are likely insensitive to North Pacific circulation effects, highlighting the paleoclimatic value of tree-ring and possibly other $\delta^{18}\text{O}$ records from this region. Our $\delta^{18}\text{O}$ -based temperature reconstruction is the first of its kind in northwestern North America, and one of few worldwide, and provides a long-term context for evaluating recent climate warming in the Mackenzie Delta region.

Keywords Mackenzie Delta · White spruce tree-rings · Stable oxygen isotope ratios · Atmospheric circulation · Temperature reconstruction · NASA-GISS ModelE

Electronic supplementary material The online version of this article (doi:10.1007/s00382-013-1674-3) contains supplementary material, which is available to authorized users.

T. J. Porter (✉)
Department of Earth and Atmospheric Sciences,
University of Alberta, Edmonton, Canada
e-mail: porter@ualberta.ca
URL: <http://www.tjporter.webs.com>

T. J. Porter · M. F. J. Pisaric · P. deMontigny
Department of Geography and Environmental Studies,
Carleton University, Ottawa, Canada

M. F. J. Pisaric
Department of Geography, Brock University, St. Catharines,
Canada

R. D. Field · R. Healy · A. N. LeGrande
NASA Goddard Institute for Space Studies, New York, USA

R. D. Field
Department of Applied Physics and Applied Mathematics,
Columbia University, New York, USA

S. V. Kokelj
Aboriginal Affairs and Northern Development Canada,
Yellowknife, Canada

T. W. D. Edwards
Department of Earth and Environmental Sciences,
University of Waterloo, Waterloo, Canada

1 Introduction

Instrumental climate records for most of the planet are limited to the last hundred years, and the duration and spatial-density of these records decrease poleward (Lawrimore et al. 2011). Improved spatiotemporal coverage of climate data is needed to better characterise the high latitude climate system, assess its sensitivity to pre-industrial forcings, and provide initialisation and verification datasets for climate models used to forecast climate changes and associated impacts. In place of missing instrumental data, natural proxies can be used to fill gaps in the global climate observing network (Jones et al. 2009; Bradley 2011).

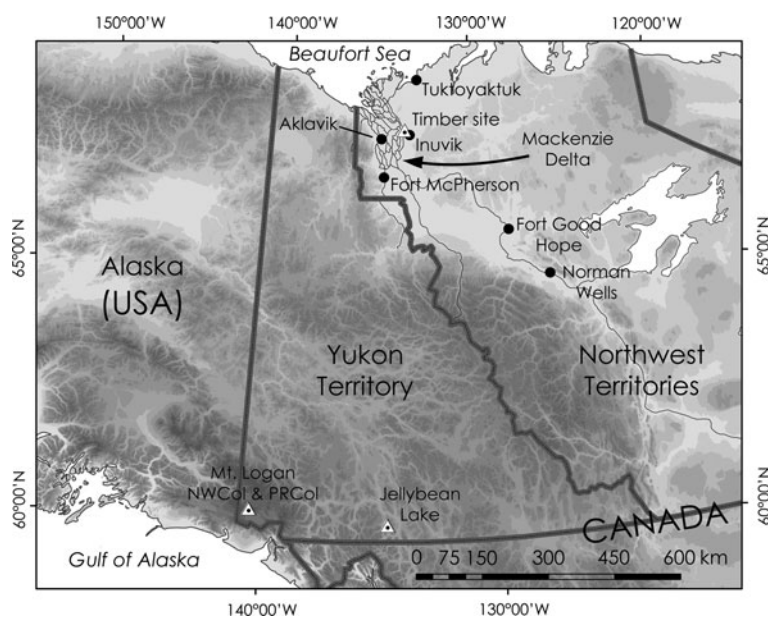
Tree-ring chronologies are especially useful because they are annually-resolved and, thus, comparable to instrumental climate records (Hughes 2011). The most climatically-sensitive tree-ring growth (e.g., ring-width or -density) chronologies are generally found at the margins of a tree's ecological range where climate is the primary limiting factor (Briffa et al. 2002). Arctic treeline is one such environment where tree-ring growth is temperature-limited and has provided valuable insights on climate over the past millennium (Esper et al. 2002; D'Arrigo et al. 2006; Wahl and Ammann 2007). However, in recent decades, some white spruce trees in northwestern Canada and Alaska have exhibited transient temperature-growth responses (Jacoby and D'Arrigo 1995; D'Arrigo et al. 2004; Wilmking et al. 2004; Pisaric et al. 2007; McGuire et al. 2010; Porter and Pisaric 2011), known as the Divergence Problem (hereafter 'divergence'; D'Arrigo et al. 2008). This issue has raised concerns over the ability to use affected ring-width chronologies for past climate reconstructions (Jansen et al. 2007).

In light of these concerns, Porter et al. (2009) explored the potential of tree-ring stable oxygen isotope ratios ($\delta^{18}\text{O}$) as an alternative proxy in the Mackenzie Delta, a region where divergence is widespread (Pisaric et al. 2007). Previous studies have demonstrated potential to use tree-ring $\delta^{18}\text{O}$ as a climate proxy (e.g., Libby and Pandolfi 1974; Gray and Thompson 1976; Barbour et al. 2001; Treydte et al. 2006; Cullen and Grierson 2007), but few have developed tree-ring $\delta^{18}\text{O}$ chronologies for long-term climate reconstructions (Gagen et al. 2011). Further, there have been few tree-ring $\delta^{18}\text{O}$ studies at higher-latitudes (e.g., Saurer et al. 2002; Sidorova et al. 2008; Hilaavuori et al. 2009; Seftigen et al. 2011) where the spatiotemporal coverage of instrumental climate data is most limiting to climate change studies.

Porter et al. (2009) developed tree-ring $\delta^{18}\text{O}$ records (AD 1850–2003) from three white spruce trees at a site in the Mackenzie Delta, unofficially named 'Timber' (Fig. 1). Timber $\delta^{18}\text{O}$ was shown to be most significantly associated with spring-summer minimum temperatures at Inuvik, the nearest station with a long-term climate record (AD 1957–2003), suggesting a first-order link to temperature-dependent isotopic labelling of local precipitation (Dansgaard 1964). However, this relation has yet to be rigorously tested for climate reconstruction purposes. The main purpose of this study is to assess the robustness of the Timber $\delta^{18}\text{O}$ -temperature signal and develop an extended temperature reconstruction for the study region if warranted.

One factor that could complicate temperature signals in tree-ring $\delta^{18}\text{O}$ or any terrestrial $\delta^{18}\text{O}$ archive that derives from meteoric water is variability in atmospheric circulation patterns (Edwards et al. 1996, 2008; Birks and

Fig. 1 Map of $\delta^{18}\text{O}$ study sites (triangles) and climate stations (solid dots) of interest. The shaded relief indicates areas of higher (dark grey) versus lower (light grey) elevation



Edwards 2009; Liu et al. 2011; Saurer et al. 2012), which can alter the source region or rain-out history of atmospheric moisture, as well as precipitation seasonality, potentially affecting the stability of temperature signals in $\delta^{18}\text{O}$ archives (Dansgaard 1964; Jouzel 1999; Sodemann et al. 2008; Sturm et al. 2010). The effects of circulation are most pronounced during winter and least during summer in the extratropics (Field 2010). Trees in the Mackenzie Delta do not grow during winter. However, soil water is a mixture of snow melt and summer rains (Mackay 1983) and, therefore, tree-ring $\delta^{18}\text{O}$ at Timber partly reflects cool-season meteoric $\delta^{18}\text{O}$ and could be influenced by atmospheric circulation (Porter et al. 2009).

The Mackenzie Delta is atmospherically downstream from the North Pacific, and the North Pacific supplies most of the water and energy advected to the study region and greater Mackenzie River Basin (Szeto et al. 2008). During the cold-season especially, most of this water is delivered by cyclonic systems from the North Pacific (Lackman and Gyakum 1996). As the annual Arctic sea ice melts during the warm season, open water in the Beaufort Sea provides an opportunity for ocean-atmosphere moisture flux and some transport inland to the study region. However, even during summer, the North Pacific is by far the most important source of moisture advected to the study region (Petroni and Rouse 2000). Therefore, factors that influence the path of North Pacific moisture to the study region potentially could have some effect on the Timber $\delta^{18}\text{O}$ -temperature relation and could complicate the interpretation of the Timber $\delta^{18}\text{O}$ record as a simple first-order temperature proxy. To a large extent, the trajectory of North Pacific moisture is determined by the semi-permanent Aleutian Low (AL) over the North Pacific (Burns 1973; Wahl et al. 1987; Dyke 2000; Serreze and Barry 2005), which varies at seasonal, inter-annual, decadal and even longer timescales (Trenberth and Hurrell 1994; Anderson et al. 2005), and is our main concern in this study. During times of strengthened AL, atmospheric circulation becomes meridional, which draws warm air into northwestern North America and results in wetter (drier) conditions on the windward (leeward) side of the Alaska-Yukon coastal mountains (Mock et al. 1998; Szeto et al. 2008); a more zonal flow pattern occurs during periods of weakened AL.

To determine if AL variability has influenced the Timber $\delta^{18}\text{O}$ -temperature relation, it is important to test the relation over a period that experienced a wide range of circulation patterns. Here, we evaluate the relation using a newly compiled regional temperature record, derived from six local datasets, that extends over the past century. Over this analysis period, AL has varied at interannual and decadal frequencies, as quantified by the North Pacific Index (NPI; Trenberth and Hurrell 1994). At least for winter-spring months, the range of NPI variability over the past century appears to be

representative of its range over the last 400 years based on a well-verified NPI reconstruction by D'Arrigo et al. (2005). Therefore, our period of temperature- $\delta^{18}\text{O}$ analysis seems appropriate for assessing the stability of the temperature- $\delta^{18}\text{O}$ relation under a wide range of circulation patterns.

However, evidence from three independent $\delta^{18}\text{O}$ records in southwestern Yukon [Fig. 1—Mt. Logan Northwest (NW) Col and Prospector Russell (PR) Col ice-cores (Holdsworth et al. 1992; Fisher et al. 2004) and Jellybean Lake sediment-core (Anderson et al. 2005)] suggests a major AL regime shift may have occurred at ca. AD 1840 that is unprecedented since at least AD 800 when a similar event is thought to have occurred (Fisher et al. 2004). From ca. AD 1600–1840, the NWCol/PRCol and Jellybean records were characterised by relatively high $\delta^{18}\text{O}$ values and lower $\delta^{18}\text{O}$ values following the event. Conversely, most biological temperature proxies in the region indicate relatively cool conditions prior to the mid-nineteenth century and warmer conditions since then (Szeicz and MacDonald 1995; Davi et al. 2003; D'Arrigo et al. 2006; Viau et al. 2012). This coarse pattern of temperature variability should have caused $\delta^{18}\text{O}$ to increase in the NWCol/PRCol and Jellybean records if they were dictated by a classical temperature effect. As such, these records were thought to be circulation-sensitive, and it was speculated that the AD 1840 shift was evidence of a shift from a zonal to meridional circulation regime, consistent with an intensified AL (Fisher et al. 2004). Simulations from an isotope-enabled general circulation model, however, suggest that enhanced meridional circulation would likely increase not decrease meteoric $\delta^{18}\text{O}$ (Field et al. 2010). Regardless, if a circulation regime shift did occur at AD 1840, it might have affected $\delta^{18}\text{O}$ archives across interior northwestern North America and the stability of $\delta^{18}\text{O}$ -temperature signals in these archives. To explore this possibility in the Mackenzie Delta, we extended the Timber $\delta^{18}\text{O}$ tree-ring record back to AD 1780 to look for anomalous variability at ca. AD 1840 as evidence of the regime shift.

Finally, we conducted simulations with the NASA-GISS ModelE isotope-enabled general circulation model (Schmidt et al. 2005, 2006) as an additional line of inquiry to better understand the potential effect of North Pacific atmospheric circulation on meteoric and tree-ring $\delta^{18}\text{O}$ in the Mackenzie Delta. This exercise also provides insights that are pertinent to site selection for $\delta^{18}\text{O}$ -based paleoclimate research in northwestern North America.

2 Materials and methods

2.1 Tree-ring $\delta^{18}\text{O}$ data

The mean climatology, site characteristics, and existing tree-ring $\delta^{18}\text{O}$ series for Timber site are described by Porter

et al. (2009). New cores from this study were sampled from white spruce trees in 2008 and 2009 using a Haglof increment borer (12 mm inner diameter). A single bark-to-bark core passing through or near the pith was collected from mature white spruce trees, providing two radii from each tree. Cores from three trees were selected for isotope analysis. The number of sample trees used in this study is low compared to most ring-width dendroclimatology studies. However, fewer independent samples are generally needed for tree-ring stable isotope studies to yield a robust mean site chronology (Gagen et al. 2011), as estimated by the expressed population signal (EPS; Wigley et al. 1984) or another measure of signal-to-noise ratio. In most tree-ring isotope studies that have assessed the inter-tree signal-to-noise ratio, 4–5 trees are often sufficient to achieve an acceptable result (Leavitt and Long 1984; Gagen et al. 2006), but a fixed number of samples cannot be prescribed for all studies due to local environmental conditions that can lead to more or less isotopic variability between trees (Leavitt 2010). In this study, only three trees were analysed since Porter et al. (2009) have already demonstrated that three white spruce trees yield a relatively high signal-to-noise ratio at Timber site. We reiterate this last point based on the EPS analysis discussed below.

Sample cores were selected on the basis of tree longevity and ring-width. Tree longevity was a criterion to ensure that the new tree-ring $\delta^{18}\text{O}$ series would extend several decades prior to the AD 1840 $\delta^{18}\text{O}$ anomaly reported by Fisher et al. (2004) in southwestern Yukon Territory. Ring-width was a criterion to ensure a sufficient sample amount for analysis. Trees at Timber have extremely narrow rings during the early-nineteenth century which was a technical challenge for separating individual rings and ensuring enough α -cellulose after processing. To overcome this challenge, cores with wider tree-rings during the problem years were preferentially selected. This same criterion was used by Porter et al. (2009) due to the narrowness of tree-rings during the late-twentieth century.

Growth patterns of the selected cores were first visually cross-dated, measured using a Velmex tree-ring measuring system, and verified against the Timber master tree-ring chronology using the computer program COFECHA (Holmes 1983). Sample rings were then separated under magnification using a scalpel. Corresponding rings from opposite radii of the same tree (i.e., representing the same year) were pooled, consistent with the sampling strategy used by Porter et al. (2009). Pooling of corresponding rings from the same tree is done in order to provide a more representative estimate of $\delta^{18}\text{O}$ for each ring, as the $\delta^{18}\text{O}$ value of a ring varies circumferentially (Leavitt 2010). This same sampling strategy is commonly used in traditional ring-width studies, but ring-width series from opposite radii are first measured independently and later combined into a mean index (Speer 2010).

Sample rings from two of the trees span the years AD 1790–1865, and AD 1780–1870 from the third tree. Samples were milled to fine wood particles, approximating the consistency of a fine sand, and processed to α -cellulose based on the method of Brendel et al. (2000) but modified to include an alkaline hydrolysis step to ensure complete removal of non- α -cellulose compounds (Gaudinski et al. 2005; Boettger et al. 2007). In contrast, the Porter et al. (2009) samples were processed using a Jayme-Wise-type α -cellulose extraction method as described by Green (1963; see also Sternberg 1989). The two methods differ in terms of oxidants used to remove hemicelluloses. However, given the same wholewood, both methods produce chemically- and isotopically-identical α -cellulose when fine-particle samples are used (Gaudinski et al. 2005).

The $\delta^{18}\text{O}$ analysis for this study was completed at the G.G. Hatch Stable Isotope Laboratory, University of Ottawa. The system specifications and reference standards used are outlined by Porter and Middlestead (2012). In contrast, Porter et al. (2009) completed their analysis at the Environmental Isotope Laboratory, University of Waterloo. Because equipment and laboratory protocols used in the two studies are not identical, $\delta^{18}\text{O}$ offsets between the two datasets can occur. A recent inter-laboratory comparison by Boettger et al. (2007) demonstrated this effect showing that $\delta^{18}\text{O}$ results for the same samples but analysed at 9 different laboratories were systematically offset by as much as 1 ‰, and this was attributed to differences in sample storage and pyrolysis temperature. A possible analytical offset between the Porter et al. (2009) and new $\delta^{18}\text{O}$ series was assessed by comparing their median chronologies over their common period of overlap (AD 1850–1870). An average offset of 0.7 ‰ was observed, likely due to inter-laboratory factors, and was corrected by adjusting the new series by +0.7 ‰ to bring them in line with the Porter et al. (2009) series. Adjusting the new series, however, is an arbitrary choice as it is difficult to say which dataset was most accurately measured with respect to Vienna Standard Mean Ocean Water (VSMOW).

To evaluate the $\delta^{18}\text{O}$ precision of the samples, Quality Assurance (QA) standards were prepared according to the identical treatment method outlined by Porter and Middlestead (2012). Fourteen QA standards were processed along with 210 of the 243 samples in equal batches (i.e., 1 QA standard + 15 samples per batch). The blanket $\delta^{18}\text{O}$ precision estimate based on these QA standards was ± 0.3 ‰, which is typical for non-processing-related uncertainties alone (McCarroll and Loader 2004). Given this result, it is likely that the samples were consistently processed to the same α -cellulose purity. In comparison, the $\delta^{18}\text{O}$ precision for the Porter et al. (2009) data was ± 0.4 ‰.

Tukey's bi-weight robust mean is commonly used in dendrochronology research when combining independent tree-ring series into a mean chronology if sample size is greater than six, and the median function is used when sample size is less than or equal to six (Cook 1985). Both measures of central tendency help to guard against outlier data points that can strongly affect the mean chronology when sample size is low. Here, sample size is always less than or equal to six, and so the median function is used to calculate the master Timber $\delta^{18}\text{O}$ chronology.

The EPS statistic (Wigley et al. 1984) was used to estimate the signal-to-noise ratio of the mean $\delta^{18}\text{O}$ chronology:

$$EPS = N \times (\overline{rbar}) \div (1 + (N - 1) \times \overline{rbar}) \quad (1)$$

where \overline{rbar} is the mean inter-series correlation between all trees over a given window length, and N is the number of series involved in the calculation. The EPS calculation used here is based on a 51-year window length. Because all Timber $\delta^{18}\text{O}$ series do not cover the same period, and some series are not internally-continuous (e.g., null data points in the 1970s due to narrow rings; refer to Porter et al. 2009), the EPS calculation was given some flexibility to allow up to a third of the 51 years for each tree to contain null data points. In these cases, N is not a discrete number and was defined as the mean number of trees available over the 51-year period.

2.2 Regional composite temperature records

Regional composite minimum, mean, and maximum temperature records (AD 1892–2010) were developed and used to assess the long-term temperature-dependence of the master Timber $\delta^{18}\text{O}$ chronology. The composite records were developed using temperature data from several local stations including Tuktoyaktuk (1970–2007), Inuvik (1957–2006), Aklavik (1926–2007), Fort McPherson (1892–1977), Fort Good Hope (1908–2007), and Normal Wells (1943–2010) (Fig. 1). Raw temperature data were downloaded from the Environment Canada website (<http://climate.weatheroffice.gc.ca>). As temperatures between stations are biased by geographic position, the mean and variance of each record were adjusted to match the Inuvik record before calculating the monthly regional means (Online Resources 1–3). The regional composite records are discontinuous from AD 1892–1909 for most months, and continuous from AD 1910–2010.

2.3 Regression model calibration and verification

Correlation analysis was used to evaluate the relation between the Timber $\delta^{18}\text{O}$ master chronology and monthly minimum, mean, and maximum temperatures. Monthly temperatures that shared a strong relation with Timber $\delta^{18}\text{O}$

were averaged into an optimal seasonal index. A linear regression model was developed for the instrumental period (AD 1892–2003), with $\delta^{18}\text{O}$ as the predictor and the optimal seasonal index (introduced in the Results and Discussion section) as the predictand. A split-period calibration/verification analysis (Cook and Kairiukstis 1990) was used to test the robustness of the temperature- $\delta^{18}\text{O}$ relation. The calibration statistics were Pearson's Product Moment Correlation Coefficient (r), the coefficient of determination (r^2), adjusted- r^2 , Standard Error (SE), Durbin-Watson (DW), and sign-test. The verification statistics were the Reduction of Error (RE) and Coefficient of Efficiency (CE). Upon successful validation of the two split-period models, regression parameters for the full calibration period were used to reconstruct temperatures back to AD 1780 based on the Timber $\delta^{18}\text{O}$ record.

2.4 Isotope-enabled general circulation modelling

The expected response between North Pacific atmospheric circulation and meteoric $\delta^{18}\text{O}$ was examined using the NASA-GISS ModelE general circulation model, which is equipped with stable water isotope tracers (Schmidt et al. 2005, 2006). The model was configured with a $2^\circ \times 2.5^\circ$ horizontal grid resolution and 40 vertical levels, a higher resolution than Field et al. (2010). Simulations were run over the 1970–2009 period with horizontal winds nudged toward the NCEP/NCAR Reanalysis (Kalnay et al. 1996) and sea surface temperatures and sea-ice prescribed from Rayner et al. (2003).

Spatial correlations between NPI (calculated as the mean sea-level pressure for the area 30°N – 65°N , 160°E – 140°W ; Trenberth and Hurrell 1994) and the modelled meteoric $\delta^{18}\text{O}$ were examined for fall-winter (Nov–Feb) and spring-summer (Apr–Jul) months. Seasonal $\delta^{18}\text{O}$ means, computed from monthly means, were weighted by monthly precipitation amount. We examined raw correlations between NPI and the meteoric $\delta^{18}\text{O}$ field, and also partial correlations between NPI and a 'residual' meteoric $\delta^{18}\text{O}$ field with the influence of temperature removed. Use of both the raw and partial correlations helped to better understand the extent to which any circulation influence could be separated from any temperature influence. Lastly, the relation between modelled precipitation amount and NPI was explored to determine the potential for changes in precipitation seasonality, which could influence the seasonal bias of bulk soil water $\delta^{18}\text{O}$ for a given site.

3 Results and discussion

3.1 Timber $\delta^{18}\text{O}$ chronology

The median $\delta^{18}\text{O}$ records from this study and Porter et al. (2009) are well correlated ($r = 0.69$, $p \leq 0.001$, one-tailed)

over the common period of overlap (AD 1850–1870), which indicates a common environmental forcing and supports combining the new and old series into a master chronology (Fig. 2). The master chronology spans the period AD 1780–2003 and is defined by one to six trees depending on the year (overall mean is 2.9 trees/year). The average sample size is low compared to most traditional dendroclimatology studies, but EPS results indicate a high signal-to-noise ratio. The mean EPS for the record is 0.86 (i.e., 86 % signal, 14 % noise), which is above the 0.85 threshold recommended by Wigley et al. (1984) for dendroclimatic research. It is noteworthy that this relatively high EPS value was obtained with only three trees for most years and, to our knowledge, this is one of only a few tree-ring $\delta^{18}\text{O}$ studies to demonstrate such a strong result with only three trees.

In another tree-ring $\delta^{18}\text{O}$ study of white spruce from the central Canadian sub-Arctic, Holzkämper et al. (2012) developed $\delta^{18}\text{O}$ series from three trees and observed mean inter-series correlations (based on a 25-year window) during the period AD 1938–2003 that varied from ca. 0.3 to 0.85, which equates to an EPS of 0.56 to 0.94. Comparatively, our EPS time-series has a range of 0.74 to 0.96 over the last two centuries. Our EPS falls slightly below 0.85 during most but not all years from AD 1896–1963. The mean EPS during this period is 0.80. The lowest EPS values occur in the mid-twentieth century. These lower values are due to the reduced sample depth during the 1970s and a period of lower inter-series coherence during the 1920s and '30s. While much of the latter half of our record falls below the $\text{EPS} = 0.85$ threshold, these reduced values are only marginally less than 0.85, indicating that the mean chronology is still of good overall quality (always greater than 75 % signal, except for 1974 with an EPS of 0.74) and warrants the use of this chronology for

paleoclimatic interpretation. However, a higher degree of caution may be required when interpreting the mid-twentieth century portion of the chronology.

3.2 Timber $\delta^{18}\text{O}$ -temperature association

Monthly (prior-year September to growth-year August) correlations between the master Timber $\delta^{18}\text{O}$ chronology and the minimum, mean, and maximum regional composite temperature records were assessed over the period AD 1892–2003 (Table 1). Consistent with the findings of Porter et al. (2009), we find that Timber $\delta^{18}\text{O}$ is most closely associated with spring-summer temperatures. However, an exception is that we find April–July are the most strongly correlated months, while Porter et al. (2009) found March–July were most important based on their analysis using the shorter Inuvik temperature record (i.e., AD 1957–2003). Based on the longer regional temperature record, we find no significant correlations with March temperatures.

In general, monthly correlations are strongest for minimum and mean temperatures. Seasonal temperature averages for April–May (AM), April–June (AMJ), and April–July (AMJJ) were correlated with Timber $\delta^{18}\text{O}$ to identify the optimal seasonal index. In each of these cases, Timber $\delta^{18}\text{O}$ was again most strongly correlated with minimum and mean temperatures, and we focus on these results. Correlations are roughly equal in strength between minimum and mean temperatures, and are strongest for AMJJ and AMJ. Split-period calibration/verification analyses were carried out to determine the seasonal index, minimum versus mean and AMJJ versus AMJ, that is most closely associated with Timber $\delta^{18}\text{O}$. The RE and sign-test statistics were used to identify the optimal temperature

Fig. 2 Statistics and time-series for the Timber $\delta^{18}\text{O}$ tree-ring data. Sample depth (no. trees), mean inter-tree correlation (rbar), and expressed population signal (EPS) are in reference to the individual tree $\delta^{18}\text{O}$ time-series below; a 20-year cubic smoothing spline with a 50 % frequency cut-off (Cook and Peters 1981) was used to highlight trends in rbar and EPS. Individual tree $\delta^{18}\text{O}$ series (light grey); median $\delta^{18}\text{O}$ values of the Porter et al. (2009) trees (black) and new trees from this study (medium grey); interpolated $\delta^{18}\text{O}$ values (black dots) for the years 1972 and 1976; master Timber chronology (lower plot, black)

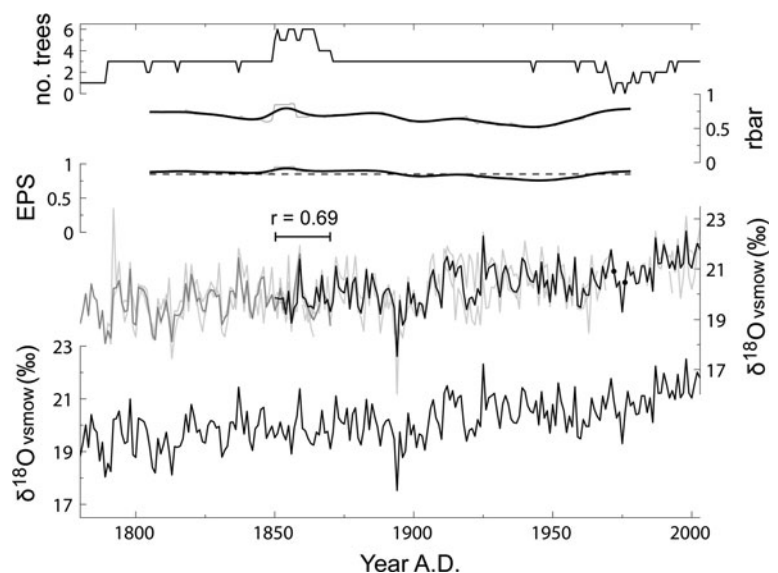


Table 1 Monthly and seasonal correlations between regional minimum, mean, and maximum temperatures and the Timber $\delta^{18}\text{O}$ chronology (AD 1892–2003)

	Min	Mean	Max
Year $t - 1$			
Sept	0.21	–	–
Oct	0.17	–	–
Nov	0.20	0.20	0.20
Dec	0.24	0.18	–
Year t			
Jan	0.23	0.19	–
Feb	0.19	–	–
Mar	0.22	–	–
Apr	0.48	0.46	0.42
May	0.44	0.43	0.39
Jun	0.32	0.35	0.34
Jul	0.27	0.22	–
Aug	–	–	–
Season			
AMJJ ^a	0.55	0.54	0.50
AMJ ^a	0.54	0.54	0.51
AM	0.52	0.50	0.47

All correlations are significant at $p \leq 0.05$ (one-tailed); correlations significant at $p \leq 0.01$ are bolded

^a For certain years from AD 1893–1908, temperature data (Online Resources 1–3) were available for April and May, and only one of June or July, but not both. To allow the calculation of April–July seasonal averages for these years, the missing June or July data points were estimated using the 4 closest years of data. For minimum, mean, and maximum temperatures, data were missing for June (1896) and July (1893, 1900, and 1908). Mean July (maximum July) temperature data were also missing for 1899 (1898 and 1899)

index. These statistics can be thought of as tests of coherence, the sign-test being specific to the high-frequency domain and RE being a more general measure of low- and high-frequency coherence. The exhaustive details of these tests are not presented here. Overall, we found that the relation between Timber $\delta^{18}\text{O}$ and AMJJ minimum temperatures was the strongest and most consistent between the split periods, and these results are presented in the following section.

Last, it is worthwhile noting that April and May appear to contribute more to the Timber $\delta^{18}\text{O}$ temperature signal than June and July given the stronger monthly correlations for April and May (Table 1), despite the fact that April and May provide only half as much precipitation to the annual water budget compared to June and July (28.3 vs. 54.3 cm, respectively) according to AD 1971–2000 climate normals (Porter et al. 2009). Three factors may explain this finding. First, April and May precipitation falls as snow, which tends to be swept by wind from tundra areas and frozen channels throughout the delta and accumulate in forested

areas due to the snow fence effect (Rouse 1984), thereby likely contributing more to the bulk soil water $\delta^{18}\text{O}$ upon melting than climate normals would suggest. Second, roughly half of all warm season precipitation in the Mackenzie River Basin is recycled from local evaporation and transpiration, and so only half of June–July precipitation is ‘new’ and advected from outside the region (Szeto et al. 2008). These two factors would tend to counter the apparent imbalance between April–May and June–July precipitation indicated by climate normals such that April–May would contribute more new water to bulk soil water than June–July. Thus, if strength of monthly temperature– $\delta^{18}\text{O}$ correlations is roughly proportional to the amount of new precipitation that falls each month, the finding that April and May are more important to the overall $\delta^{18}\text{O}$ –temperature signal compared to June and July would seem to make sense. Third, there is also the possibility that meteoric $\delta^{18}\text{O}$ is more sensitive to temperatures during April–May than June–July, since the temperature– $\delta^{18}\text{O}$ relation for many parts of the world can vary seasonally (Fricke and O’Neil 1999). However, the lack of long-term meteoric $\delta^{18}\text{O}$ records for this area precludes a direct assessment of this possibility.

3.3 Regression model calibration and verification

The robustness of the April–July minimum temperature– $\delta^{18}\text{O}$ relation was evaluated by a linear regression split-period calibration/verification analysis (Table 2). The calibration periods were 1893–1953 (Split 1) and 1954–2003 (Split 2), and the verification periods were opposite the calibration periods. Timber $\delta^{18}\text{O}$ explains 35 and 16 % of temperature variability for Splits 1 and 2, respectively. The weaker adjusted- r^2 for Split 2 is probably due to the fact that the master chronology is not as well defined during the 1970s and ‘80s due to low sample depth; the mean chronology is defined by 3 trees for Split 1, and 2.2 trees for Split 2. The DW statistic is close to a value of 2.0 during Splits 1 and 2, indicating low autocorrelation in the residuals. The standard error is lower for Split 1 (1.05 °C) compared to Split 2 (1.36 °C), indicating more error in the Split 2 residuals, as would be expected given the sample depth differences. Results for the sign-test, a high-frequency test, are mixed. The Split 1 sign-test result is highly significant indicating that the sign of interannual $\delta^{18}\text{O}$ changes closely matches corresponding changes in April–July minimum temperature. However, Split 2 does not pass the sign-test. Again, this likely relates to the lower sample depth during Split 2. Despite this result, it is encouraging that Timber $\delta^{18}\text{O}$ is associated with temperatures as strongly as it is considering the many potential sources of non-temperature-related noise, including analytical uncertainties (Werner and Brand 2001; Porter and Middlestead 2012), secondary

evaporative-enrichment effects (Roden et al. 2000; Porter et al. 2009), residual soil water from previous years and occasional flooding (Kokelj and Burn 2005), and uncertainty in the meteoric $\delta^{18}\text{O}$ -temperature association (Dansgaard 1964; Fricke and O'Neil 1999).

The fact that the calibration diagnostics were not exactly the same between Split 1 and Split 2 indicates that the temperature- $\delta^{18}\text{O}$ relation is not perfectly stable. However, it is perhaps unrealistic to expect a perfectly stable relation given the changes in sample depth between the two periods and possible overprinting of the climate signal by various sources of analytical and environmental noise, as discussed above. The positive RE and CE statistics indicate that both of the calibration models are predictively-superior to the mean climatologies of the calibration and verification periods, respectively. This result provides some evidence that the temperature- $\delta^{18}\text{O}$ relation is relatively stable and suitable for reconstruction purposes. Further evidence to support this claim is presented below. A full-period (AD 1893–2003) model was calibrated, explaining 29 % of observed temperature variability (Table 2). This level of temperature- $\delta^{18}\text{O}$ co-variability is comparable to observations from other high-latitude tree-ring studies (e.g., $r^2 = 0.21$ to 0.47 —Sidorova et al. 2008; Csank et al. 2011; Seftigen et al. 2011; Holzkämper et al. 2012). A similar range of co-variability has been reported for other white spruce ring-width or -density studies in northwestern North America (e.g., $r^2 = 0.29$ – 0.49 —Szeicz and MacDonald

1995; Barber et al. 2004; Youngblut and Luckman 2008; Anchukaitis et al. 2012).

The full-period calibration model is characterised by a DW statistic of 1.97, a standard error of 1.24 °C, and a sign-test of 60 agreements and 40 disagreements ($p \leq 0.057$) (Table 2). A more detailed analysis of residuals was used to determine if the full period model conforms to standard regression model assumptions. Several null hypotheses were tested: (1) the residuals are not normally distributed (Lilliefors test); (2) the residuals are not homoscedastic (2-sample F-test for equal variances, based on first and second halves of the calibration period); and (3) residuals are proportional to predicted values (regression slope test). Each null hypothesis was rejected at the $p \leq 0.05$ significance level, indicating that the temperature- $\delta^{18}\text{O}$ relation does not violate these critical regression model assumptions.

A visual comparison of observed versus predicted temperatures (Fig. 3) provides strong evidence that the temperature- $\delta^{18}\text{O}$ relation was relatively stable during the instrumental period. 'Local' temperatures in the comparison are from the regional instrumental data (Online Resource 1). We also used gridded temperature data from the Twentieth Century V2 Reanalysis (20CR) project (Compo et al. 2011) as additional verification. The 20CR data are generated from a numerical weather prediction model constrained by observed surface pressure, sea-surface temperatures, and sea-ice extent. For the study region and neighbouring areas (60 – 70°N , 130 – 140°W), the 20CR April–July temperatures approximate local temperatures reasonably well (Online Resource 4) and were used to fill gaps in the local temperature record from AD 1871–1909.

Predicted and local-20CR temperatures are well matched from AD 1871–2003 (Fig. 3). This coherence is especially strong at lower-frequencies (e.g., $r = 0.78/0.88$ if both series are smoothed with a 5-year/10-year cubic-smoothing spline; Cook and Peters 1981). From AD 1871–1893, both records show a brief cooling to a low in AD 1893, warming to the ca. 1940s, slight cooling to the ca. 1960s, and a further warming trend to present. Qualitatively, it is encouraging that the reconstruction captures the AD 1893 cooling event, but it does not fully capture the AD 1998 warm event coinciding with the 1997/98 El-Niño (Van Oldenborgh 2000) that had a major effect on global climate. However, given the many sources of noise that could influence the tree-ring $\delta^{18}\text{O}$ -temperature signal, it is not surprising that some extreme events are not well predicted. Overall, this comparison demonstrates a relatively stable temperature- $\delta^{18}\text{O}$ relation. Based on the visual and statistical diagnostics presented, we conclude that Timber $\delta^{18}\text{O}$ is a valid temperature proxy and use the full-period regression model to reconstruct April–July minimum

Table 2 Calibration/verification and full-period (AD 1893–2003) calibration statistics for linear regression models of April–July minimum temperatures as a function of the mean Timber $\delta^{18}\text{O}$ chronology

	Split 1	Split 2	Full period
Calibration			
Period	1893–1953	1954–2003	1893–2003
N	51 ^a	50	101
Slope	0.97	0.87	1.01
Intercept	–23.60	–20.92	–24.10
SE	1.05	1.36	1.24
DW	1.47	2.19	1.97
r	0.60	0.42	0.55
r ²	0.37	0.17	0.30
Adjusted-r ²	0.35	0.16	0.29
Sign (+/-)	36/14 [§]	23/26	60/40*
Verification period			
Period	1954–2003	1893–1953	n/a
N	50	51 ^a	n/a
RE	0.31	0.46	n/a
CE	0.08	0.21	n/a

^a The period 1893–1909 contains only 51 years of valid data points due to missing temperature data; sign-test results significant at [§] $p \leq 0.01$ and * $p \leq 0.1$; all correlation results are significant at $p \leq 0.01$ (one-tailed)

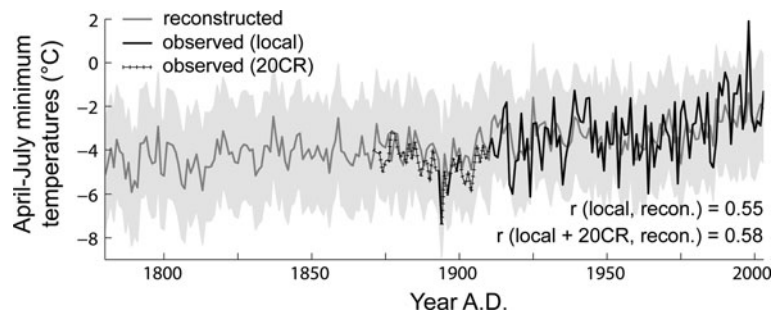


Fig. 3 Comparison between observed and reconstructed April–July minimum temperatures since AD 1871. Observed temperature data are a composite of the local and Twentieth Century Reanalysis

(20CR) temperature data. The shaded confidence interval represents two standard errors of the estimate (± 2.48 °C). All correlations are significant at $p \leq 0.001$ (one-tailed)

temperatures since AD 1780 (Fig. 3). The reconstruction is discussed in the following section.

On a final note about the relative stability of the temperature- $\delta^{18}\text{O}$ relation, this finding also provides indirect support for the idea that Timber $\delta^{18}\text{O}$ has been insensitive to recent North Pacific circulation variability. Over the twentieth century, NPI varied considerably at interannual and decadal timescales, especially in winter-spring months (Trenberth and Hurrell 1994). In spite of this variability, the $\delta^{18}\text{O}$ -temperature relation was found to be relatively stable overall (Fig. 3). Additional empirical support for this idea is gained by comparing April–July temperature- $\delta^{18}\text{O}$ correlations between two periods defined by the upper ($r = 0.46$, $2\sigma = 0.20$, $p \leq 0.05$) and lower ($r = 0.38$, $2\sigma = 0.22$, $p \leq 0.05$) 50th percentiles ranked by April–July NPI. There is no significant difference in April–May temperature- $\delta^{18}\text{O}$ correlations between periods of high versus low NPI. The implied insensitivity of Timber $\delta^{18}\text{O}$ to North Pacific atmospheric circulation may relate to the spring-summer seasonal bias of Timber $\delta^{18}\text{O}$ and the fact that extratropical meteoric $\delta^{18}\text{O}$ is less sensitive to atmospheric circulation during the warm-season than the cool-season (Field 2010). Another possibility is that the seasonality of precipitation contributing to Timber $\delta^{18}\text{O}$ is insensitive to North Pacific circulation effects. Both possibilities are later evaluated using the ModelE simulations.

Assuming that the modern range of North Pacific atmospheric circulation was typical of the past several centuries, as indicated by the D'Arrigo et al. (2005) NPI reconstruction, and the principle causes of variability in temperature and meteoric $\delta^{18}\text{O}$ have been relatively constant, it may be reasonable to assume the Timber $\delta^{18}\text{O}$ -temperature relation was also time-stable over the reconstruction period, AD 1780–2003. However, circulation patterns were likely very different over longer Holocene timescales due to changes in insolation, boreal treeline, and sea ice extent (Burn 1997), and these have had marked effects on $\delta^{18}\text{O}$ archives in other regions (Edwards et al.

1996; Hammarlund et al. 2002). As the stability of the Timber $\delta^{18}\text{O}$ -temperature relation over these longer timescales is not well known, the development and paleoclimatic interpretation of Holocene-scale tree-ring $\delta^{18}\text{O}$ records from this region should be guided by additional research on this key uncertainty. Isotope-enabled general circulation models forced by known changes in Holocene boundary conditions offer one means of addressing this uncertainty (LeGrande and Schmidt 2007; Sturm et al. 2010).

3.4 Timber $\delta^{18}\text{O}$ -temperature reconstruction

According to the reconstruction, April–July minimum temperatures in the Mackenzie Delta region today are the warmest they have been in the last 230 years, which agrees with ring-width- and ring-density-based summer temperature reconstructions from Alaska, Yukon, and Northwest Territories (Szeicz and MacDonald 1995; D'Arrigo et al. 2006; Anchukaitis et al. 2012), as well as multi-proxy site networks at the circumpolar (Overpeck et al. 1997; Kaufman et al. 2009) and hemispheric (Mann et al. 2008) scales. The reconstructed mean temperature for the most recent 30-year period (AD 1974–2003) is -2.8 °C. By comparison, the coolest portion of the reconstruction occurs during the early nineteenth century, corresponding with the Dalton Minimum, a period of reduced insolation (Bard et al. 2000) and increased volcanism (Gao et al. 2008). The period AD 1787–1816 had the lowest 30-year reconstructed average of -4.6 °C. This cool period is well replicated by many ring-width- and ring-density-based temperature reconstructions across the Northern Hemisphere (Briffa 2000; Luckman and Wilson 2005; D'Arrigo et al. 2006), and is linked to societal hardship (settlement abandonment, trans-Atlantic migration and war) in Europe (Büntgen et al. 2011). Over the 224-year reconstruction, April–July minimum temperatures for the Mackenzie Delta warmed by ca. $+0.08$ °C/decade or a total of ca. $+1.8$ °C.

3.5 The AD 1840 event

Based on the Timber $\delta^{18}\text{O}$ chronology (Fig. 2), we find no evidence of a major $\delta^{18}\text{O}$ shift in the Mackenzie Delta at ca. AD 1840. The Timber chronology exhibits a gradual rising trend from AD 1780 to the late-nineteenth century. There are no shifts from enriched to depleted values in the mid-nineteenth century, as were found in the NWCol/PRCol (Holdsworth et al. 1992; Fisher et al. 2004) and Jellybean Lake (Anderson et al. 2005) records. One fluctuation in the Timber $\delta^{18}\text{O}$ record that is a departure from normal variability is the dip in AD 1893, but this is related to low temperatures recorded in the instrumental data (Fig. 3). Assuming Timber $\delta^{18}\text{O}$ is an archive for meteoric $\delta^{18}\text{O}$, these results appear to suggest that no large-scale North Pacific circulation regime shift occurred at AD 1840, or that meteoric $\delta^{18}\text{O}$ and precipitation seasonality in the Mackenzie Delta were unaffected by the shift.

As discussed above, the relatively stable relation between Timber $\delta^{18}\text{O}$ and April–July minimum temperatures since AD 1871 (Fig. 3) provides indirect support for the idea that Timber $\delta^{18}\text{O}$ is insensitive to North Pacific atmospheric circulation changes. We further evaluate this idea with the ModelE simulations, examining the influence of North Pacific circulation effects on meteoric $\delta^{18}\text{O}$ and precipitation amount (Fig. 4) under the idealized conditions of a GCM.

Results vary between November–February (NDJF) and April–July (AMJJ), as would be expected since North Pacific atmospheric circulation patterns vary widely between the cool- and warm-seasons (Serreze and Barry 2005), but generalizations can be made. First we consider the raw NPI- $\delta^{18}\text{O}$ results (Fig. 4, left side). For NDJF, there are pronounced and inverse correlations along coastal Yukon near NWCol/PRCol and Jellybean Lake, indicating that a strengthened AL (i.e., enhanced meridional flow) would cause an increase in meteoric $\delta^{18}\text{O}$, as was suggested by Field et al. (2010). Because the annual water budget for this area is cold-season biased (as per the NCEP/NCAR Reanalysis; Kalnay et al. 1996), it seems likely that a shift in the NWCol/PRCol and Jellybean Lake $\delta^{18}\text{O}$ records would occur given a major shift in North Pacific atmospheric circulation. Conversely, raw NDJF correlations are insignificant for Timber site and generally insignificant for nearby areas. However, the AMJJ season is more relevant to Timber $\delta^{18}\text{O}$ given its spring-summer bias (Porter et al. 2009). The raw AMJJ NPI- $\delta^{18}\text{O}$ results reveal no significant correlation for Timber, supporting the notion that meteoric and tree-ring $\delta^{18}\text{O}$ in the Mackenzie Delta is likely to be insensitive to North Pacific atmospheric circulation variability.

Absent the effects of temperature, the partial NPI- $\delta^{18}\text{O}$ correlations (Fig. 4, center) provide important insights into

the nature of circulation effects. For southwestern Yukon, the partial NDJF correlation results show weakened and non-significant correlations, in contrast with the raw results discussed above. This difference implies that much of the raw circulation effect for this region is mediated by temperature, consistent with a first-order Rayleigh interpretation (Dansgaard 1964). However, some of the raw circulation effect along coastal Yukon cannot be accounted for by temperature and, thus, can be attributed to changes in source region and/or rain-out history. In the Mackenzie Delta, the partial NPI- $\delta^{18}\text{O}$ correlation results for NDJF and AMJJ show no significant correlations. Again, the AMJJ result is likely most relevant for identifying potential circulation-related complications to the Timber $\delta^{18}\text{O}$ -temperature signal. Overall, these results suggest meteoric and tree-ring $\delta^{18}\text{O}$ in the Mackenzie Delta are unlikely to be sensitive to North Pacific atmospheric circulation variability.

For Timber, NPI-precipitation correlations are generally weak and insignificant for NDJF and AMJJ, but with a greater number of significant NDJF correlations for adjacent areas (Fig. 4, right; see also Online Resource 5 for a longer-term NPI-precipitation amount correlation analysis using the NCEP/NCAR [1948–2009; Kalnay et al. 1996] and ERA-40 [1958–2002; Uppala et al. 2005] Reanalysis datasets, which provides additional support for the ModelE results). Again, the AMJJ correlations are most important for Timber due to the spring-summer bias of the region's water budget. Overall, the lack of any strong NPI-precipitation correlations for this area suggests that precipitation amount and, indirectly, precipitation seasonality are insensitive to North Pacific circulation effects. Considering the NPI-precipitation and NPI- $\delta^{18}\text{O}$ results in tandem, it seems unlikely that North Pacific atmospheric circulation variability would strongly affect soil water or tree-ring $\delta^{18}\text{O}$ in the Mackenzie Delta, implying that the Timber $\delta^{18}\text{O}$ record is of considerable value as a temperature proxy. Given this result, the absence of the AD 1840 shift in the Timber $\delta^{18}\text{O}$ record should not be considered as evidence that a major North Pacific circulation regime change did not occur, as the Timber $\delta^{18}\text{O}$ record is probably insensitive to these events.

As for southwestern Yukon, a significant and inverse NDJF NPI-precipitation correlation is observed for NWCol/PRCol, but not Jellybean Lake, suggesting a stronger AL would cause increased precipitation for NWCol/PRCol (Fig. 4, right). However, based on the NCEP/NCAR Reanalysis data (Online Resources 5), NPI does have a significant influence on precipitation at Jellybean Lake during NDJF. No significant AMJJ NPI-precipitation correlations are observed for NWCol/PRCol or Jellybean Lake. Because the annual water budget for this region is cold-season biased, a North Pacific circulation

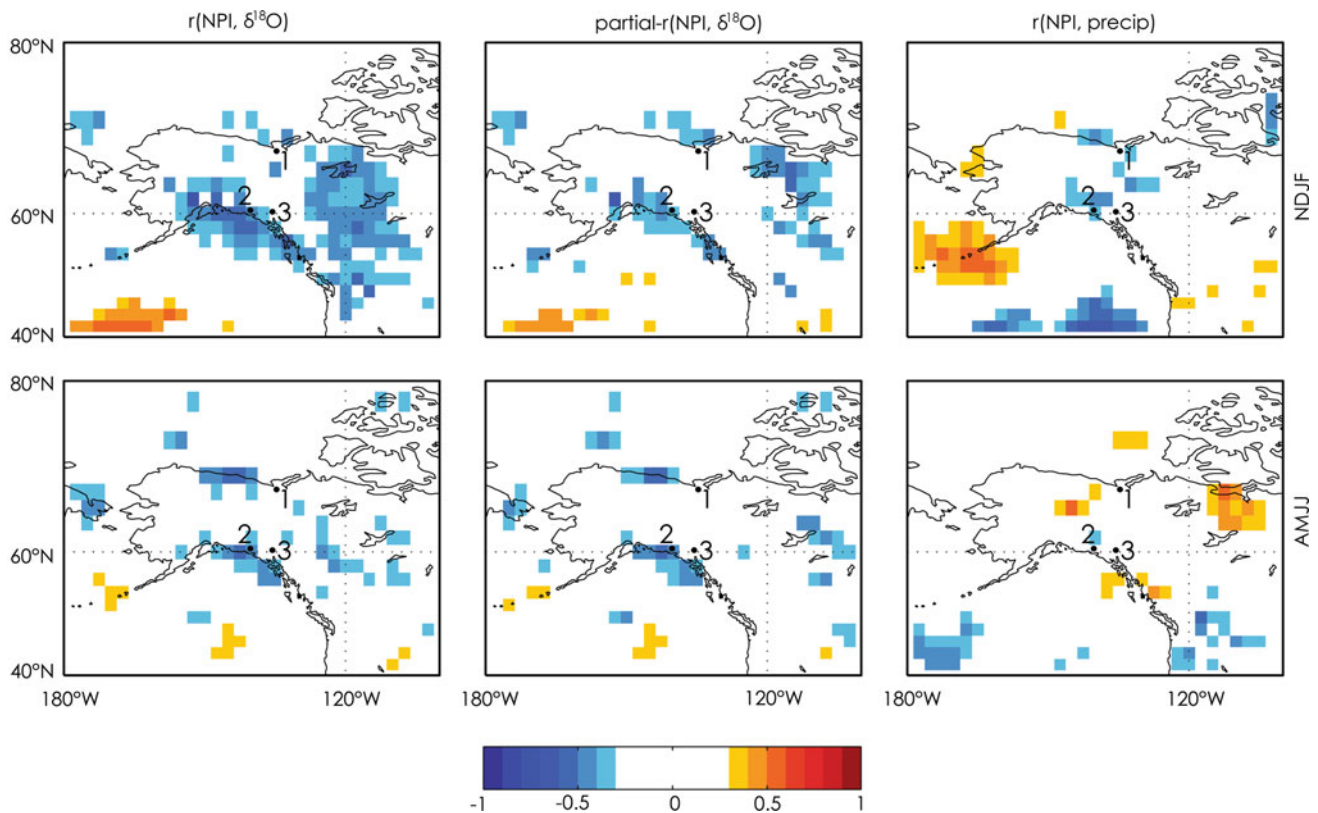


Fig. 4 Correlation between NPI and simulated climate fields for fall-winter (NDJF; *top*) and spring-summer (AMJJ; *bottom*) for the period 1970–2009. The simulated climate fields are the raw meteoric $\delta^{18}\text{O}$ field (*left*), a residual meteoric $\delta^{18}\text{O}$ field—*influence of temperature removed* (*center*), and the precipitation amount field (*right*). Correlations are significant at $p \leq 0.05$ (two-tailed; n.b., not adjusted for

autocorrelation). Points 1, 2, and 3 are Timber, NWCol/PRCol, and Jellybean Lake, respectively. NPI-precipitation amount correlations were also assessed using the longer NCEP/NCAR (1948–2009; Kalnay et al. 1996) and ERA-40 (1958–2002; Uppala et al. 2005) reanalysis datasets (Online Resource 5)

regime shift might be expected to induce a change in precipitation seasonality (i.e., ratio of cold- to warm-season precipitation amount). As such, the AD 1840 shift from enriched to depleted $\delta^{18}\text{O}$ in the NWCol/PRCol and Jellybean Lake records could represent an increase in the ratio of cold- to warm-season precipitation amount, possibly due to enhanced meridional flow as was proposed by Fisher et al. (2004). Together, the NPI- $\delta^{18}\text{O}$ and NPI-precipitation results indicate that the net circulation-driven response in $\delta^{18}\text{O}$ archives in southwestern Yukon is complex due to opposing effects of moisture source/trajectory and precipitation seasonality, which cancel to some extent. A more sophisticated analysis would be required to determine which factor is likely to dominate in this region, but that is beyond the scope of this study.

4 Concluding remarks

Previous studies have explored the paleoclimatic potential of tree-ring $\delta^{18}\text{O}$ for various locales around the world (McCarroll and Loader 2004, and references therein), but

nearly all were limited to the modern instrumental period. By comparison, there are few examples of long tree-ring isotope chronologies developed for reconstruction purposes, a chief criticism of Gagen et al. (2011). Tree-ring $\delta^{18}\text{O}$ has been used for quantitative climate reconstructions, but there are few explicit temperature reconstructions worldwide. One example is from Ellesmere Island in the Canadian High Arctic where Csank et al. (2011; see also Ballantyne et al. 2006, 2010) used fossil tree-rings to infer more than 200 years of temperature variability during the early Pliocene. Another example is from the eastern Rocky Mountains of western Canada where Edwards et al. (2008) coupled tree-ring $\delta^{13}\text{C}$ and $\delta^{18}\text{O}$ to resolve temperature and relative humidity signals over the past millennium. And a third example is from the eastern Rocky Mountains of Colorado where Berkelhammer and Stott (2012) reconstructed temperatures from tree-ring $\delta^{18}\text{O}$ for the period AD 1485-present. Here we have demonstrated the first tree-ring $\delta^{18}\text{O}$ -based temperature reconstruction for a high-latitude site in northwestern North America. The statistical and visual diagnostics of our reconstruction provide strong evidence that tree-ring $\delta^{18}\text{O}$ is a viable climate proxy for

the Mackenzie Delta region and offers promise for much longer-term reconstructions since millennial-length tree-ring chronologies are known to exist in this region (Szeicz and MacDonald 1996; Bégin et al. 2000).

It is important to acknowledge that our reconstruction explains only 29 % of interannual temperature variability, although low-frequency trends can be more reliably predicted. In future studies, a higher level of interannual variability may be explained with improved sample depth. Sample depth during the calibration period was especially low during the 1970s and '80s due to extremely narrow rings shared by most trees at Timber during this interval, which precluded an adequate amount of α -cellulose for isotope analysis since only two radii were sampled from each tree. The lower sample depth during this interval may have contributed to a lower coefficient of determination for the Timber $\delta^{18}\text{O}$ -temperature relation. However, it is unclear how much more variability can be explained simply by augmenting sample depth, as the $\delta^{18}\text{O}$ -temperature signal is also overprinted by various sources of analytical and environmental noise. For future studies in the Mackenzie Delta and other regions where slow-growing trees are found, the challenge of ensuring enough α -cellulose for the analysis could be easily overcome by sampling four or more radii from each tree and pooling corresponding rings into annual samples.

The fact that the Timber $\delta^{18}\text{O}$ -temperature signal is more strongly associated with spring (April–May) compared to summer (June–July) temperatures also deserves attention. For high-latitude boreal sites, traditional tree-ring indicators such as ring-width are often biased towards summer temperatures (Garfinkel and Brubaker 1980; Jacoby and D'Arrigo 1989; Briffa et al. 1998; Barber et al. 2000; Davi et al. 2003; Wilson et al. 2007; D'Arrigo et al. 2009; Esper et al. 2010; Andreu-Hayles et al. 2011), which imparts a summer bias on large-scale reconstructions that are based heavily on ring-width. While seasonal differences (e.g., warm- vs. cold-season) are less important over multi-decadal to centennial time-scales (Jones et al. 2009), there is a need for proxies with a variety of seasonal biases in order to improve knowledge of seasonal and annual climate dynamics at regional- and global-scales. Improved knowledge of seasonal dynamics could serve several purposes including the ability to provide refined training datasets for climate models, and diagnosing the natural origins of climate anomalies. At least in the Mackenzie Delta, tree-ring $\delta^{18}\text{O}$ responds to a broader seasonal window of climate than tree-ring width (Bégin et al. 2000; Pisaric et al. 2007) and, together, these proxies can potentially be used to tease apart differences between spring and summer conditions.

The well-known relation between temperature and meteoric $\delta^{18}\text{O}$, especially for higher-latitude sites, presents

an obvious opportunity to use $\delta^{18}\text{O}$ archives to reconstruct temperatures. This relation has been most popularly applied to the Greenland and Antarctica ice-cores (Jouzel et al. 1987; Dansgaard et al. 1993; Johnsen et al. 2001; Augustin et al. 2004), but atmospheric circulation variability can complicate the interpretation of $\delta^{18}\text{O}$ archives as first-order proxies for temperature (Sturm et al. 2010). The importance of these effects for most parts of the world is not yet well understood, partly due to the paucity of the global meteoric $\delta^{18}\text{O}$ records (Bowen and Revenaugh 2003). However, as we demonstrated here, isotope-enabled GCMs can be used as practical tools for understanding the importance of circulation effects for various regions, and it would seem there is potential to use these models to guide in site selection for tree-ring $\delta^{18}\text{O}$ research. For example, if the research objective is to develop a temperature reconstruction, areas where circulation effects are expected to be strong should be avoided. Conversely, if circulation is the target variable, areas that are most strongly affected by circulation could be sampled.

Acknowledgments Financial support for this project is gratefully acknowledged: Aboriginal Affairs and Northern Development Canada grant; NSERC Discovery grant and Northern Supplement (M. Pisaric); Northern Scientific Training Program (T. Porter); NSERC Postgraduate Scholarship (T. Porter). Resources supporting this work were provided by the NASA High-End Computing (HEC) Program through the NASA Center for Climate Simulation (NCCS) at Goddard Space Flight Center. We also thank two anonymous reviewers for their helpful comments which improved the final manuscript.

References

- Anchukaitis K, D'Arrigo R, Andreu-Hayles L et al (2012) Tree-ring reconstructed summer temperatures from northwestern North America during the last nine centuries. *J Clim*. doi:10.1175/JCLI-D-11-00139.1
- Anderson L, Abbott MB, Finney BP, Burns SJ (2005) Regional atmospheric circulation change in the North Pacific during the Holocene inferred from lacustrine carbonate oxygen isotopes, Yukon Territory, Canada. *Quat Res* 64:21–35
- Andreu-Hayles L, D'Arrigo R, Anchukaitis KJ, Beck PSA, Frank D, Goetz S (2011) Varying boreal forest response to Arctic environmental change at the Firth River, Alaska. *Environ Res Lett* 6. doi:10.1088/1748-9326/6/4/045503
- Augustin L, Barbante C, Barnes PRF et al (2004) Eight glacial cycles from an Antarctic ice core. *Nature* 429:623–628
- Ballantyne AP, Rybczynski N, Baker PA, Harrington CR, White D (2006) Pliocene Arctic temperature constraints from the growth rings and isotopic composition of fossil larch. *Palaeogeogr Palaeoclimatol Palaeoecol* 242:188–200
- Ballantyne AP, Greenwood DR, Sinnighe-Damsté JS, Csank AZ, Eberle JJ, Rybczynski N (2010) Significantly warmer Arctic surface temperatures during the Pliocene indicated by multiple independent proxies. *Geology* 38:603–606
- Barber VA, Juday GP, Finney BP (2000) Reduced growth of Alaskan white spruce in the twentieth century from temperature-induced drought stress. *Nature* 405:668–673

- Barber VA, Juday GP, Finney BP, Wilmking M (2004) Reconstruction of summer temperatures in interior Alaska from tree-ring proxies: evidence for changing synoptic climate regimes. *Clim Chang* 63:91–120
- Barbour MM, Andrews TJ, Farquhar GD (2001) Correlations between oxygen isotope ratios of wood constituents of *Quercus* and *Pinus* samples from around the world. *Aust J Plant Physiol* 28:335–348
- Bard E, Raisbeck G, Yiou F, Jouzel J (2000) Solar irradiance during the last 1200 years based on cosmogenic nuclides. *Tellus B* 52:985–992
- Bégin C, Michaud Y, Archambault S (2000) Tree-ring evidence of recent climate changes in the Mackenzie Basin, Northwest Territories. *Geological Survey of Canada Bulletin* 547:65–77
- Berkelhammer M, Stott LD (2012) Secular temperature trends for the southern Rocky Mountains over the last five centuries. *Geophys Res Lett* 39. doi:10.1029/2012GL052447
- Birks SJ, Edwards TWD (2009) Atmospheric circulation controls on precipitation isotope-climate relations in western Canada. *Tellus B* 61:566–576
- Boettger T, Haupt M, Knöller K et al (2007) Wood cellulose preparation methods and mass spectrometric analyses of $\delta^{13}\text{C}$, $\delta^{18}\text{O}$, and nonexchangeable $\delta^2\text{H}$ values in cellulose, sugar, and starch: an interlaboratory comparison. *Anal Chem* 79:4603–4612
- Bowen GJ, Revenaugh J (2003) Interpolating the isotopic composition of modern meteoric precipitation. *Water Resour Res* 39. doi:10.1029/2003WR002086
- Bradley RS (2011) High-resolution paleoclimatology. In: Hughes MK, Swetnam TW, Diaz H (eds) *Dendroclimatology: progress and prospects*. Springer, New York, pp 3–15
- Brendel O, Iannetta PPM, Stewart D (2000) A rapid and simple method to isolate pure alpha-cellulose. *Phytochem Anal* 11:7–10
- Briffa KR (2000) Annual climate variability in the Holocene: interpreting the message of ancient trees. *Quat Sci Rev* 19:87–105
- Briffa KR, Schweingruber FH, Jones PD, Osborn TJ, Shiyatov SG, Vaganov EA (1998) Reduced sensitivity of recent tree-growth to temperature at high northern latitudes. *Nature* 391:678–682
- Briffa KR, Osborn TJ, Schweingruber FH, Jones PD, Shiyatov SG, Vaganov EA (2002) Tree-ring width and density data around the Northern Hemisphere: part 1, local and regional climate signals. *Holocene* 12:737–757
- Büntgen U, Tegel W, Nicolussi K et al (2011) 2500 years of European climate variability and human susceptibility. *Science* 331:578–582
- Burn CR (1997) Cryostratigraphy, paleogeography, and climate change during the early Holocene warm interval, western Arctic coast, Canada. *Can J Earth Sci* 34:912–925
- Burns BM (1973) *The climate of the Mackenzie Valley-Beaufort Sea*. Environment Canada, Toronto
- Compo GP, Whitaker JS, Sardeshmukh PD et al (2011) The Twentieth Century Reanalysis Project. *Q J Royal Meteorol Soc* 137:1–28
- Cook ER (1985) A time series analysis approach to tree ring standardization. PhD dissertation. University of Arizona, Tuscon
- Cook ER, Kairiukstis LA (1990) *Methods of dendrochronology: applications in the environmental sciences*. Kluwer Academic Publishers, Boston
- Cook ER, Peters K (1981) The smoothing spline: a new approach to standardizing forest interior tree-ring width series for dendroclimatic studies. *Tree-Ring Bull* 41:45–53
- Csank AZ, Patterson WP, Eglington BM, Rybczynski N, Basinger JF (2011) Climate variability in the Early Pliocene Arctic: annually resolved evidence from stable isotope values of sub-fossil wood, Ellesmere Island, Canada. *Palaeogeogr Palaeoclimatol Palaeoecol* 308:339–349
- Cullen LE, Grierson PF (2007) A stable oxygen, but not carbon, isotope chronology of *Callitris columellaris* reflects recent climate change in north-western Australia. *Clim Chang* 85:213–229
- D'Arrigo R, Kaufmann RK, Davi N et al (2004) Thresholds for warming-induced growth decline at elevational tree line in the Yukon Territory, Canada. *Glob Biogeochem Cycles* 18. doi:10.1029/2004GB002249
- D'Arrigo R, Wilson R, Deser C et al (2005) Tropical-North Pacific climate linkages over the past four centuries. *J Clim* 18:5253–5265
- D'Arrigo R, Wilson R, Jacoby G (2006) On the long-term context for late twentieth century warming. *J Geophys Res* 111. doi:10.1029/2005JD006352
- D'Arrigo R, Wilson R, Liepert B, Cherubini P (2008) On the “Divergence Problem” in northern forests: a review of the tree-ring evidence and possible causes. *Glob Planet Chang* 60:289–305
- D'Arrigo R, Jacoby G, Buckley B et al (2009) Tree growth and inferred temperature variability at the North American arctic treeline. *Glob Planet Chang* 65:71–82
- Dansgaard W (1964) Stable isotopes in precipitation. *Tellus* 16:436–468
- Dansgaard W, Johnsen SJ, Gundestrup NS et al (1993) Evidence for general instability of past climate from a 250-kyr ice-core record. *Nature* 364:218–220
- Davi NK, Jacoby GC, Wiles GC (2003) Boreal temperature variability inferred from maximum latewood density and tree-ring width data, Wrangell Mountain region, Alaska. *Quat Res* 60:252–262
- Dyke LD (2000) Climate of the Mackenzie River valley. In: Dyke LD, Brooks GR (eds) *The physical environment of the Mackenzie Valley, Northwest territories: a baseline for the assessment of environmental change*. Geological Survey of Canada, Ottawa
- Edwards TWD, Wolfe BB, MacDonald GM (1996) Influence of changing atmospheric circulation on precipitation $\delta^{18}\text{O}$ -temperature relations in Canada during the Holocene. *Quat Res* 46:211–218
- Edwards TWD, Birks SJ, Luckman BH, MacDonald GM (2008) Climatic and hydrologic variability during the past millennium in the eastern Rocky Mountains and northern Great Plains of western Canada. *Quat Res* 70:188–197
- Esper J, Cook ER, Schweingruber FH (2002) Low-frequency signals in long tree-ring chronologies for reconstructing past temperature variability. *Science* 295:2250–2253
- Esper J, Frank D, Büntgen U, Verstege A, Hantemirov RM, Kirilyanov AV (2010) Trends and uncertainties in Siberian indicators of 20th century warming. *Glob Chang Biol* 16:386–398
- Field RD (2010) Observed and modeled controls on precipitation $\delta^{18}\text{O}$ over Europe: From local temperature to the Northern Annular Mode. *J Geophys Res* 115. doi:10.1029/2009JD013370
- Field RD, Moore GWK, Holdsworth G, Schmidt GA (2010) A GCM-based analysis of circulation controls on $\delta^{18}\text{O}$ in the southwest Yukon, Canada: Implications for climate reconstructions in the region. *Geophys Res Lett* 37. doi:10.1029/2009GL041408
- Fisher DA, Wake C, Kreutz K et al (2004) Stable isotope records from Mount Logan, Eclipse ice cores and nearby Jellybean Lake. Water cycle of the North Pacific over 2000 years and over five vertical kilometers: sudden shifts and tropical teleconnections. *Géog Phys Quatern* 58:337–352
- Fricke HC, O'Neil JR (1999) The correlation between $^{18}\text{O}/^{16}\text{O}$ ratios of meteoric water and surface temperature: its use in investigating terrestrial climate change over geologic time. *Earth Planet Sci Lett* 170:181–196
- Gagen M, McCarroll D, Edouard J-L (2006) Combining ring width, density and stable carbon isotope proxies to enhance the climate

- signal in tree-rings: an example from the Southern French Alps. *Clim Chang* 78:363–379
- Gagen M, McCarroll D, Loader NJ, Robertson I (2011) Stable isotopes in dendroclimatology: moving beyond “potential”. In: Hughes MK, Swetnam TW, Diaz HF (eds) *Dendroclimatology: progress and prospects*. Springer, New York, pp 147–172
- Gao C, Robock A, Ammann C (2008) Volcanic forcing of climate over the past 1500 years: An improved ice core-based index for climate models. *J Geophys Res* 113. doi:10.1029/2008JD010239
- Garfinkel HL, Brubaker LB (1980) Modern climate-tree-growth relationships and climatic reconstruction in sub-Arctic Alaska. *Nature* 286:872–874
- Gaudinski JB, Dawson TE, Quideau S et al (2005) Comparative analysis of cellulose preparation techniques for use with ^{13}C , ^{14}C , and ^{18}O isotopic measurements. *Anal Chem* 77:7212–7224
- Gray J, Thompson P (1976) Climatic information from $^{18}\text{O}/^{16}\text{O}$ ratios of cellulose in tree rings. *Nature* 262:481–482
- Green JW (1963) Wood cellulose. In: Whistler RL (ed) *Methods in carbohydrate chemistry, III*. Academic Press, New York, pp 9–21
- Hammarlund D, Barnekow L, Birks HJB, Buchardt B, Edwards TWD (2002) Holocene changes in atmospheric circulation recorded in the oxygen-isotope stratigraphy of lacustrine carbonates from northern Sweden. *Holocene* 12:339–351
- Hilasvuori E, Berninger F, Sonninen E, Tuomenvirta H, Jungner H (2009) Stability of climate signal in carbon and oxygen isotope records and ring width from Scots pine (*Pinus sylvestris* L.) in Finland. *J Quat Sci* 24:469–480
- Holdsworth G, Krouse HR, Nosal M (1992) Ice core climate signals from Mount Logan, Yukon, A.D. 1700–1987. In: Bradley RS, Jones PD (eds) *Climate since A.D. 1500*. Routledge, London, pp 483–504
- Holmes RL (1983) Computer-assisted quality control in tree-ring dating and measurement. *Tree-Ring Bull* 43:69–78
- Holzkaemper S, Tillman PK, Kuhry P, Esper J (2012) Comparison of stable carbon and oxygen isotopes in *Picea glauca* tree rings and *Sphagnum fuscum* moss remains from subarctic Canada. *Quat Res* 78:295–302
- Hughes MK (2011) Dendroclimatology in high-resolution paleoclimatology. In: Hughes MK, Swetnam TW, Diaz HF (eds) *Dendroclimatology: progress and prospects*. Springer, New York, pp 17–34
- Jacoby GC, D’Arrigo R (1989) Reconstructed northern hemisphere annual temperature since 1671 based on high-latitude tree-ring data from North America. *Clim Chang* 14:39–59
- Jacoby GC, D’Arrigo RD (1995) Tree ring width and density evidence of climatic and potential forest change in Alaska. *Global Biogeochem Cycles* 9:227–234
- Jansen E, Overpeck J, Briffa KR et al (2007) Palaeoclimate. In: Solomon S, Qin D, Manning M et al (eds) *Climate change 2007: the physical science basis. Contribution of working group I to the fourth assessment report of the intergovernmental panel on climate change*. Cambridge University Press, Cambridge, pp 433–497
- Johnsen SJ, Dahl-Jensen D, Gundestrup N et al (2001) Oxygen isotope and palaeotemperature records from six Greenland ice-core stations: Camp Century, Dye-3, GRIP, GISP2, Renland and NorthGRIP. *J Quat Sci* 16:299–307
- Jones PD, Briffa KR, Osborn TJ et al (2009) High-resolution palaeoclimatology of the last millennium: a review of current status and future prospects. *Holocene* 19:3–49
- Jouzel J (1999) Calibrating the isotopic paleothermometer. *Science* 286:910–911
- Jouzel J, Lorius C, Petit JR et al (1987) Vostok ice core: a continuous isotope temperature record over the last climatic cycle (160,000 years). *Nature* 329:403–408
- Kalnay E, Kanamitsu M, Kistler R et al (1996) The NCEP/NCAR 40-Year Reanalysis Project. *Bull Am Meteorol Soc* 77:437–471
- Kaufman DS, Schneider DP, McKay NP et al (2009) Recent warming reverses long-term Arctic cooling. *Science* 325:1236–1239
- Kokelj SV, Burn CR (2005) Near-surface ground ice in sediments of the Mackenzie Delta, Northwest Territories, Canada. *Permafrost Periglacial Process* 16:291–303
- Lackman GM, Gyakum JR (1996) The synoptic- and planetary-scale signatures of precipitating systems over the Mackenzie River Basin. *Atmos Ocean* 34:647–674
- Lawrimore JH, Menne MJ, Gleason BE et al. (2011) An overview of the Global Historical Climatology Network monthly mean temperature data set, Version 3. *J Geophys Res* 116. doi:10.1029/2011JD016187
- Leavitt SW (2010) Tree-ring C–H–O isotope variability and sampling. *Sci Total Environ* 408:5244–5253
- Leavitt SW, Long A (1984) Sampling strategy for stable carbon isotope analysis of tree-rings in pine. *Nature* 311:145–147
- LeGrande AN, Schmidt GA (2007) Sources of Holocene variability of oxygen isotopes in paleoclimate archives. *Clim Past* 5:441–455
- Libby LM, Pandolfi LJ (1974) Temperature dependence of isotope ratios in tree rings. *Proc Natl Acad Sci USA* 71:2482–2486
- Liu Z, Kennedy CD, Bowen GJ (2011) Pacific/North American teleconnection controls on precipitation isotope ratios across the contiguous United States. *Earth Planet Sci Lett* 310:319–326
- Luckman BH, Wilson RJS (2005) Summer temperatures in the Canadian Rockies during the last millennium: a revised record. *Clim Dynam* 24:131–144
- Mackay JR (1983) Downward water movement into frozen ground, western arctic coast, Canada. *Can J Earth Sci* 20:120–134
- Mann ME, Zhang Z, Hughes MK et al (2008) Proxy-based reconstructions of hemispheric and global surface temperature variations over the past two millennia. *Proc Natl Acad Sci USA* 105:13252–13257
- McCarroll D, Loader NJ (2004) Stable isotopes in tree rings. *Quat Sci Rev* 23:771–801
- McGuire AD, Ruess RW, Lloyd A, Yarie J, Clein JS, Juday GP (2010) Vulnerability of white spruce tree growth in interior Alaska in response to climate variability: dendrochronological, demographic, and experimental perspectives. *Can J For Res* 40:1197–1209
- Mock CJ, Bartlein PJ, Anderson PM (1998) Atmospheric circulation patterns and spatial climatic variations in Beringia. *Int J Climatol* 18:1085–1104
- Overpeck J, Hughen KA, Hardy D et al (1997) Arctic environmental change of the last four centuries. *Science* 278:1251–1256
- Petrone RM, Rouse WR (2000) Synoptic controls on the surface energy and water budgets in sub-arctic regions of Canada. *Int J Climatol* 20:1149–1165
- Pisarcic MFJ, Carey SK, Kokelj S V, Youngblut D (2007) Anomalous 20th century tree growth, Mackenzie Delta, Northwest Territories, Canada. *Geophys Res Lett* 34. doi:10.1029/2006GL029139
- Porter TJ, Middlestead P (2012) On estimating the precision of stable isotope ratios in processed tree-rings. *Dendrochronologia* 30:239–242
- Porter TJ, Pisarcic MFJ (2011) Temperature-growth divergence in white spruce forests of Old Crow Flats, Yukon Territory, and adjacent regions of northwestern North America. *Glob Chang Biol* 17:3418–3430
- Porter TJ, Pisarcic MFJ, Kokelj SV, Edwards TWD (2009) Climatic signals in $\delta^{13}\text{C}$ and $\delta^{18}\text{O}$ of tree-rings from white spruce in the Mackenzie Delta region, northern Canada. *Arct Antarct Alp Res* 41:497–505
- Rayner NA, Parker DE, Horton EB et al. (2003) Global analyses of sea surface temperature, sea ice, and night marine air

- temperature since the late nineteenth century. *J Geophys Res* 108. doi:[10.1029/2002JD002670](https://doi.org/10.1029/2002JD002670)
- Roden JS, Lin G, Ehleringer JR (2000) A mechanistic model for interpretation of hydrogen and oxygen isotope ratios in tree-ring cellulose. *Geochim Cosmochim Acta* 64:21–35
- Rouse WR (1984) Microclimate at Arctic tree line, 1. Radiation balance of tundra and forest. *Water Resour Res* 20:57–66
- Saurer M, Schweingruber FH, Vaganov EA, Shiyatov SG, Siegwolf R (2002) Spatial and temporal oxygen isotope trends at the northern tree-line in Eurasia. *Geophys Res Lett* 29. doi:[10.1029/2001GL013739](https://doi.org/10.1029/2001GL013739)
- Saurer M, Kress A, Leuenberger M, Rinne KT, Treydte KS, Siegwolf RTW (2012) Influence of atmospheric circulation patterns on the oxygen isotope ratio of tree rings in the Alpine region. *J Geophys Res* 117. doi:[10.1029/2011JD016861](https://doi.org/10.1029/2011JD016861)
- Schmidt GA, Hoffmann G, Shindell DT, Hu Y (2005) Modeling atmospheric stable water isotopes and the potential for constraining cloud processes and stratosphere-troposphere water exchange. *J Geophys Res* 110. doi:[10.1029/2005JD005790](https://doi.org/10.1029/2005JD005790)
- Schmidt GA, Ruedy R, Hansen JE et al (2006) Present-day atmospheric simulations using GISS ModelE: comparison to in situ, satellite, and reanalysis data. *J Clim* 19:153–192
- Seftigen K, Linderholm HW, Loader NJ, Liu Y, Young GHF (2011) The influence of climate on $^{13}\text{C}/^{12}\text{C}$ and $^{18}\text{O}/^{16}\text{O}$ ratios in tree ring cellulose of *Pinus sylvestris* L. growing in the central Scandinavian Mountains. *Chem Geol* 286:84–93
- Serreze MC, Barry RG (2005) The arctic climate system. Cambridge University Press, Cambridge
- Sidorova OV, Siegwolf RTW, Saurer M, Naurzbaev MM, Vaganov EA (2008) Isotopic composition ($\delta^{13}\text{C}$, $\delta^{18}\text{O}$) in wood and cellulose of Siberian larch trees for early Medieval and recent periods. *J Geophys Res* 113. doi:[10.1029/2007JG000473](https://doi.org/10.1029/2007JG000473)
- Sodemann H, Schweirz C, Wernli H (2008) Interannual variability of Greenland winter precipitation sources: Lagrangian moisture diagnostic and North Atlantic Oscillation influence. *J Geophys Res* 113. doi:[10.1029/2007JD008503](https://doi.org/10.1029/2007JD008503)
- Speer JH (2010) Fundamentals of tree-ring research. University of Arizona Press, Tucson
- Sternberg LSL (1989) Oxygen and hydrogen isotope measurements in plant cellulose analysis. In: Linskens HF, Jackson JF (eds) Modern methods of plant analysis: plant fibers. Springer, New York, pp 89–99
- Sturm C, Zhang Q, Noone D (2010) An introduction to stable water isotopes in climate models: benefits of forward proxy modelling for paleoclimatology. *Clim Past* 6:115–129
- Szeicz JM, MacDonald GM (1995) Dendroclimatic reconstruction of summer temperatures in northwestern Canada since A.D. 1638 based on age-dependent modelling. *Quat Res* 44:257–266
- Szeicz JM, MacDonald GM (1996) A 930-year ring-width chronology from moisture-sensitive white spruce (*Picea glauca* Moench) in northwestern Canada. *Holocene* 6:345–351
- Szeto KK, Stewart RE, Yau MK, Gyakum J (2008) The Mackenzie climate system: a synthesis of MAGS atmospheric research. In: Woo M (ed) Cold region atmospheric and hydrologic studies: the Mackenzie GEWEX experience. Volume 1: atmospheric dynamics. Springer, New York, pp 23–50
- Trenberth KE, Hurrell JW (1994) Decadal atmosphere-ocean variations in the Pacific. *Clim Dynam* 9:303–319
- Treydte KS, Schleser GH, Helle G et al (2006) The twentieth century was the wettest period in northern Pakistan over the past millennium. *Nature* 440:1179–1182
- Uppala SM, Kållberg PW, Simmons AJ et al (2005) The ERA-40 re-analysis. *Q J Royal Meteorol Soc* 131:2961–3012
- Van Oldenborgh GJ (2000) What caused the onset of the 1997–98 El Niño? *Mon Weather Rev* 128:2601–2607
- Viau AE, Ladd M, Gajewski K (2012) The climate of North America during the past 2000 years reconstructed from pollen data. *Glob Planet Chang* 84–85:75–83
- Wahl ER, Ammann CM (2007) Robustness of the Mann, Bradley, Hughes reconstruction of Northern Hemisphere surface temperatures: examination of criticisms based on the nature and processing of proxy climate evidence. *Clim Chang* 85:33–69
- Wahl HE, Fraser DB, Harvey RC, Maxwell JB (1987) Climate of Yukon. Climatological studies, vol 40. Environment Canada, Ottawa
- Werner RA, Brand WA (2001) Referencing strategies and techniques in stable isotope ratio analysis. *Rapid Commun Mass Spec* 15:501–519
- Wigley TML, Briffa KR, Jones PD (1984) On the average value of correlated time series, with applications in dendroclimatology and hydrometeorology. *J Climat App Meteorol* 23:201–213
- Wilmking M, Juday GP, Barber VA, Zald HSJ (2004) Recent climate warming forces contrasting growth responses of white spruce at treeline in Alaska through temperature thresholds. *Glob Chang Biol* 10:1724–1736
- Wilson R, D'Arrigo R, Buckley B et al (2007) A matter of divergence: Tracking recent warming at hemispheric scales using tree ring data. *J Geophys Res* 112. doi:[10.1029/2006JD008318](https://doi.org/10.1029/2006JD008318)
- Youngblut D, Luckman B (2008) Maximum June–July temperatures in the southwest Yukon over the last 300 years reconstructed from tree rings. *Dendrochronologia* 25:153–166